The EMBO Journal Vol. 20 No. 15 pp. 4076–4087, 2001

The Ras-like GTPase Gem is involved in cell shape remodelling and interacts with the novel kinesin-like protein KIF9

Eugenia Piddini[1,2], Johannes A.Schmid[3], Rainer de Martin[3] and Carlos G.Dotti[1,2,4]

[1]EMBL, Cell Biology and Biophysics Programme, Meyerhofstrasse 1, 69117 Heidelberg, Germany, [3]Department of Vascular Biology and Thrombosis Research, University of Vienna, Vienna International Research Cooperation Centre, A-1235 Vienna, Austria and [4]Cavaliere Ottolenghi Scientific Institute, Università degli Studi di Torino A.O. San Luigi Gonzaga Regione Gonzole, 10, I-10043 Orbassano (TO), Italy

[2]Corresponding authors
e-mail: carlos.dotti@unito.it or piddini@embl-heidelberg.de

E.Piddini and J.A.Schmid contributed equally to this work

Gem belongs to the Rad/Gem/Kir (RGK) subfamily of Ras-related GTPases, which also comprises Rem, Rem2 and Ges. The RGK family members Ges and Rem have been shown to produce endothelial cell sprouting and reorganization of the actin cytoskeleton upon overexpression. Here we show that high intracellular Gem levels promote profound changes in cell morphology and we investigate how this phenotype arises dynamically. We also show that this effect requires intact microtubules and microfilaments, and that Gem is associated with both cytoskeletal components. In order to investigate the mechanisms of Gem recruitment to the cytoskeleton, we performed a yeast two-hybrid screen and identified a novel kinesin-like protein, termed KIF9, as a new Gem interacting partner. We further show that Gem and KIF9 interact by co-immunoprecipitation. Furthermore, Gem and KIF9 display identical patterns of gene expression in different tissues and developmental stages. The Gem–KIF9 interaction reported here is the first molecular link between RGK family members and the microtubule cytoskeleton.

Keywords: actin/cell morphology/GTPases/kinesin/microtubules

Introduction

The Ras superfamily of low molecular weight GTPases is classified into six major subgroups comprising the Ras, Rho, Rab, Ran, Arf and RGK families (Bourne *et al*., 1991; Finlin *et al*., 2000). The latter group is a novel subfamily termed after the GTPases Rad and Gem/Kir (RGK). In spite of the similarities between Ras and RGK GTPases (Figure 1A), RGK family members differ from other Ras-like GTPases in a number of characteristic features (Reynet and Kahn, 1993; Cohen *et al*., 1994; Maguire *et al*., 1994). First, RGK GTPases exhibit significant modifications within certain domains such as the G3 domain, which participates in binding and hydrolysis of GTP, and the G2 region, which is involved in the binding of effector proteins. Secondly, RGK members contain notable N-terminal and C-terminal extensions over the Ras-like core region. The C-terminal extension includes a calmodulin binding region, thereby linking these GTPases to calcium signaling events (Fischer *et al*., 1996; Moyers *et al*., 1997). The N-terminal extension is likely to have regulatory functions, both for binding of calmodulin to the C-terminus and for subcellular localization (Moyers *et al*., 1997). Thirdly, RGK proteins do not have classical lipid modification motifs at the C-terminus, which are important for membrane anchorage of other Ras-like proteins (Reynet and Kahn, 1993; Cohen *et al*., 1994; Maguire *et al*., 1994; Bilan *et al*., 1998). Fourthly, RGK family members are transcriptionally regulated, a feature uncommon in other Ras-like GTPases, and exhibit tissue-specific expression patterns. Rad, which was the first representative of this emerging family of GTPases to be identified, is upregulated in skeletal muscle cells of type II diabetes patients compared with cells from normal individuals (Reynet and Kahn, 1993). Gem was shown to be upregulated in mitogen-activated T cells (Maguire *et al*., 1994) and in endothelial cells activated by IL-1, tumour necrosis factor (TNF)α or lipopolysaccharides (LPS) (Vanhove *et al*., 1997). Kir, which is identical or highly related to Gem as they share 98.4% nucleotide identity in their coding region, was discovered by a differential display screening for being overexpressed in pre-B lymphoid cells transformed by the *bcr-abl* oncogene (Cohen *et al*., 1994). The novel RGK family member Rem was instead found to be repressed after LPS administration (Finlin and Andres, 1997). Thus, RGK family members differ not only from other Ras-like GTPases, but also from each other, as they have different expression patterns and are regulated in distinct ways.

Attempts to clarify the physiological roles of RGK family members have focused on the search for effector molecules and regulatory proteins, such as GTPase activating proteins (GAPs) or kinases that phosphorylate these GTPases. The only RGK-specific GAP identified so far (Zhu *et al*., 1995, 1999) is the tumour metastasis suppressor nm23, which acts specifically on Rad but not on Gem. Strikingly, nm23 also acts as guanine-nucleotide exchange factor (GEF) and exerts this function not only on Rad, but also on Gem and even on Ras (Zhu *et al*., 1999). Several kinases have also been found to act as RGK family protein regulators by phosphorylating serine and threonine residues, predominantly near the C-terminus. One of these kinases is the calmodulin-dependent kinase II (CAMKII), which was shown to phosphorylate both Rad and Gem *in vitro* and to co-immunoprecipitate with Rad (Moyers *et al*., 1997). Rad is also a substrate for *in vitro* phosphorylation by protein kinase A (PKA), protein kinase C (PKC) and casein kinase II at specific serine residues (Moyers *et al*., 1998). Although many of the

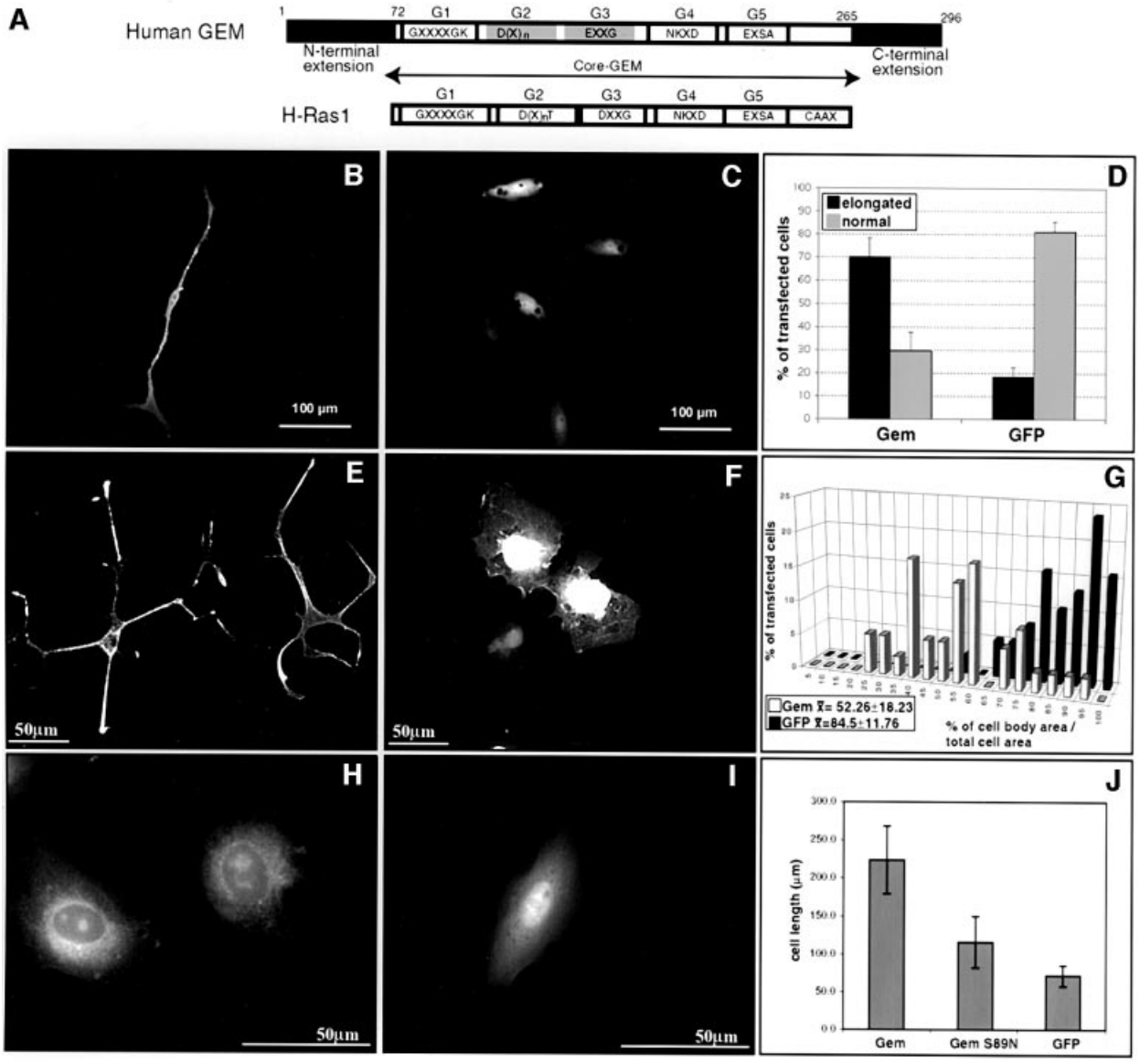

Fig. 1. Overexpression of Gem causes cell elongation in HUVEC and COS cells. (**A**) Schematic representation of Gem protein and its similarities to H-Ras 1. (**B** and **C**) HUVEC were transfected with either GFP–Gem (B) or GFP alone (C), and then fixed and visualized through GFP fluorescence. (**D**) The recurrence of the sprouting effect is quantified both for cells treated as in (B) (Gem) and as in (C) (control). Cells with a ratio between the longest and the shortest diameter exceeding a value of four were scored as 'elongated', all the others as 'normal'. (**E** and **F**) COS cells transfected with either Flag-Gem (E) or GFP (F) constructs were fixed and then either processed for immunofluorescence with an anti-Flag antibody (E), or simply visualized through GFP fluorescence (F). (**G**) A random population of transfected cells was taken from the experiments described in (E) and (F). The percentage of the total cell area covered by the cell body area (*x*-axis in the plot) was calculated for each cell, and the frequency with which each value was encountered in the sample populations was plotted as a histogram. The corresponding mean values are indicated on the lower left corner. (**H** and **I**) HUVEC were transfected with either a GemS89N/GFP construct (H) or with a GFP vector alone (I), and then visualized through GFP fluorescence. (**J**) Quantification of the cellular elongation induced by Gem, GemS89N and GFP overexpression.

putative serine phosphorylation sites are also conserved in Gem, it is not known whether they are really phosphorylated. However, it has been shown that Gem contains phosphorylated tyrosine residues, which might play a role in its regulation (Maguire *et al*., 1994).

Although the functions of this family of proteins are largely unknown, several lines of evidence suggest a link between some RGK proteins and the cytoskeleton. Rad exhibits not only a membrane and a cytosolic distribution, but also an association with cytoskeletal elements (Bilan *et al*., 1998; Moyers *et al*., 1997), although neither the nature of the cytoskeletal components to which it binds nor the molecular mechanisms of such association are known. However, hints on the mechanisms of Rad recruitment to the cytoskeleton come from the finding that this GTPase interacts with β-tropomyosin in a guanine nucleotide- and calcium-dependent manner (Zhu *et al*., 1996). A role in cytoskeleton rearrangement has been described for the RGK protein Ges and for the closely related Rem, which may represent the murine orthologue of human Ges. These GTPases promote endothelial cell sprouting and reorganization of the actin cytoskeleton (Pan *et al*., 2000).

Although not directly demonstrated, Gem/Kir function may also be linked to the cytoskeleton, as suggested by

two observations: (i) overexpression of Kir induced an elongated cell shape and pseudohyphal growth in *Saccharomyces cerevisiae* (Dorin *et al*., 1995) and (ii) Kir was found to be overexpressed in fully malignant versus growth factor-independent pre-B cell lines (Cohen *et al*., 1994), as well as in tumour-derived cell lines (Ross *et al*., 2000). In this study, we report that Gem plays a role in cellular morphology using a machinery that requires intact microtubules and microfilaments. We report for the first time that an RGK protein interacts with the microtubule cytoskeleton, and provide a new Gem interacting partner, the kinesin-like protein KIF9, as a candidate molecule responsible for such cytoskeletal association.

Results

Gem overexpression promotes the formation of long cellular processes

In order to gain insight into the function of the RGK family member Gem, we studied the cellular effects of its overexpression. Human umbilical vein endothelial cells (HUVEC) were transiently transfected with Flag-tagged Gem or green fluorescent protein (GFP)-tagged Gem, and processed for immunofluorescence. Cells overexpressing GFP–Gem exhibited a clear alteration of the normal morphology with a significant elongation and a spindle-like appearance (Figure 1B). This effect was also observed with the Flag-Gem construct (not shown), whereas GFP-expressing control cells showed no change in morphology (Figure 1C). Quantification of this phenomenon revealed a statistically significant difference between control and Gem-expressing cells (Figure 1D).

To understand whether the Gem effect on cellular morphology was specific to endothelial cells, we tested the sensitivity of other cell types to high intracellular levels of the Gem protein. COS cells were transfected with either a Flag-Gem- or a GFP- (control) expressing construct, and the cell shape was analysed 18 h afterwards. Just as observed for HUVEC, Gem overexpression in COS cells caused severe morphological changes: the cell body area appeared reduced and cells had formed unusually long processes, acquiring a dendritic-like appearance (Figure 1E). Such a phenotype was not encountered in control GFP-transfected cells (Figure 1F). To confirm that the recurrence of this effect was statistically relevant, we measured it in 40 randomly chosen GFP alone or Flag-Gem expressing cells. The central cell body area/total cell area ratio was taken as a measure of cell elongation; lower values corresponded to increased cell elongation. As is shown in the histogram in Figure 1G, both the distribution profile and the mean value obtained for Gem over-expressing cells were markedly shifted towards lower ratios compared with the control cells. Similar results were obtained in Chinese hamster ovary (CHO) and HEK-293 cells (data not shown).

Nucleotide binding was required for the full elongation activity of Gem, since GemS89N, bearing a single point mutation in the GTP-binding site that is predicted to lock the protein in a nucleotide-free state with high affinity for its GEF (Feig, 1999), was significantly less active than wild-type Gem, both in HUVEC (Figure 1H–J) and in COS cells (data not shown).

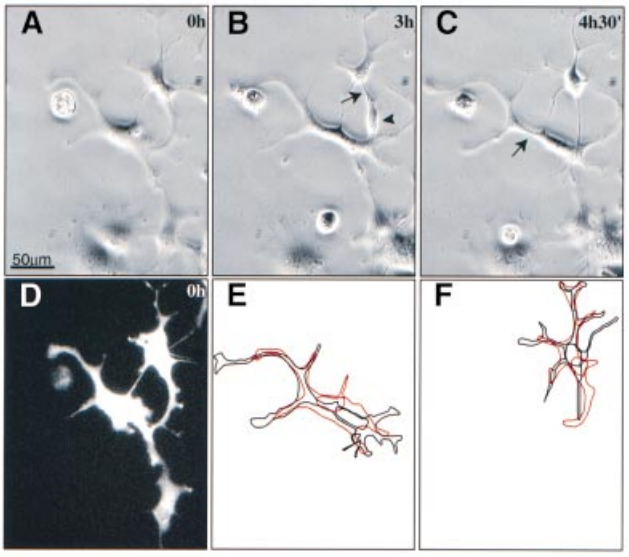

Fig. 2. Dynamics of Gem-induced cellular elongation. COS cells transiently expressing GFP–Gem were followed by time-lapse video microscopy for several hours. (**A**–**C**) Frames selected at the indicated time points from a representative movie. Arrows in (B) and (C) point at sites of cortical contraction. The arrowhead in (B) indicates the new position of the nucleus. (**D**) Fluorescence image taken at the same time point as in (A). Cells transfected by GFP–GEM can be identified. (**E** and **F**) Schematic representations of the morphological changes that the cells in the centre and at the top right, respectively, underwent. The drawings in red represent the initial cell shapes as seen in (A); the drawings in black represent the final cell shapes as seen in (C).

The dynamics of Gem-mediated formation of long cellular processes

The mechanism by which Gem-induced cellular projections arise was analysed in more detail by time-lapse video microscopy. COS cells transiently expressing GFP–Gem were imaged for 2–5 h until they acquired the elongated phenotype described above. Figure 2A–C shows three frames, at different time points, selected from a representative movie. Two cells that expressed high levels of GFP–Gem are seen (Figure 2D). These two cells (centre and top right) acquired a markedly elongated morphology over time (compare Figure 2A with 2B and C). The cell in the centre did so by moving its cell body (nucleus and surrounding cytoplasm) down to the right, while its processes on the left, instead of trailing behind, kept on growing in the opposite direction (Figure 2E). The cell at the top right, instead, retracted its cell body while it elongated pre-existing processes and created new ones, thereby acquiring a spider-like appearance (Figure 2F).

Moreover, Gem-expressing cells displayed an abnormal nuclear motility. An extreme case is exemplified by the cell at the top right, whose nucleus abandoned the cell centre, migrated down to the end of one of the processes (arrowhead in Figure 2B) and returned back to its position at later times (Figure 2C). Another feature encountered in Gem-overexpressing cells was the occurrence of abnormal cortical contraction events, which could be due to an increased actomyosin activity (arrows in Figure 2B and C). The Gem-induced phenotype was observed only in cells that expressed high levels of exogenous Gem; cells expressing low levels of GFP–Gem behaved normally (bottom right corner of Figure 2D).

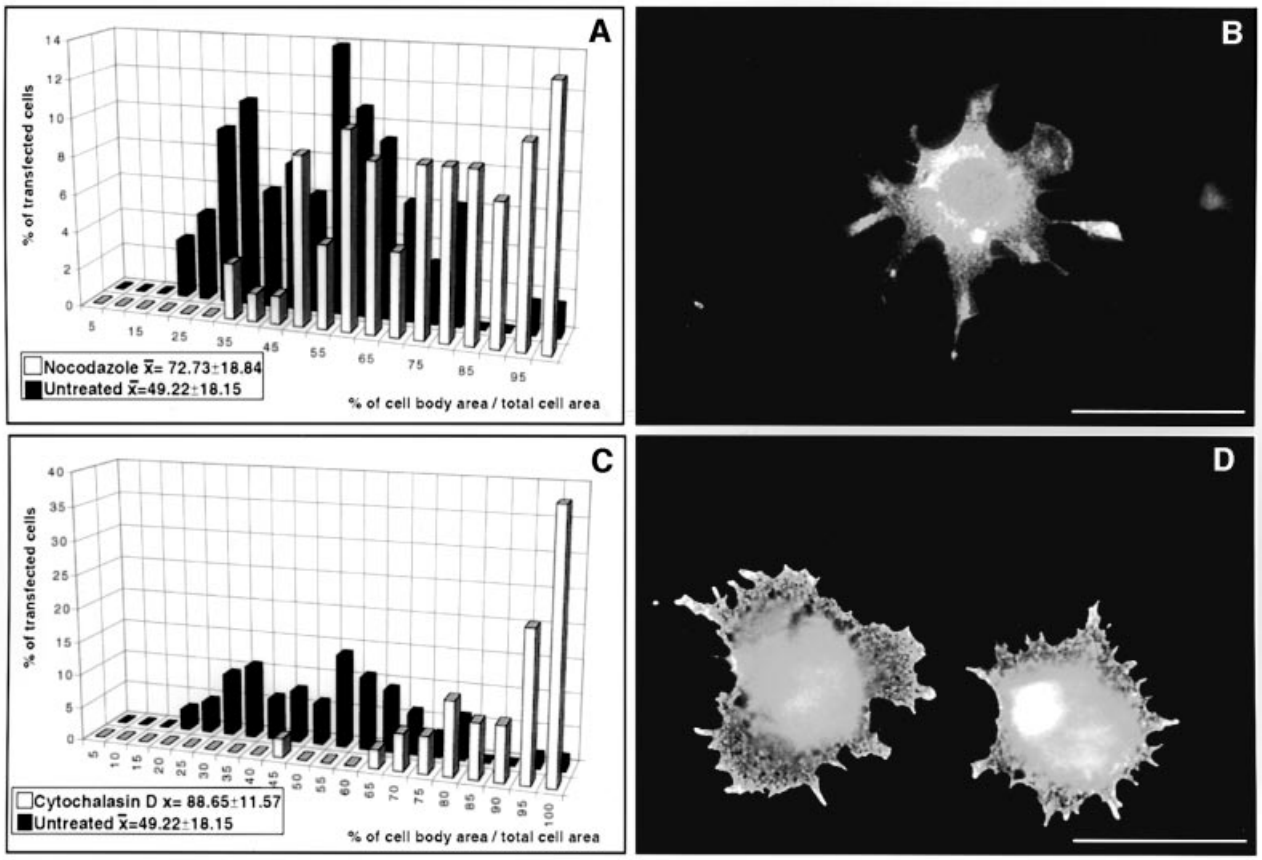

Fig. 3. Microtubules or actin depolymerization inhibit Gem-induced cell spreading. Flag-Gem transfected COS cells were incubated overnight either with 10 μM nocodazole (**A** and **B**), or 1 μg/ml cytochalasin D (**C** and **D**), or left untreated and then fixed and processed for immunofluorescence with an anti-Flag antibody. (B) and (D) show representative Gem-overexpressing cells after nocodazole or cytochalasin D treatment, respectively (scale bars: 50 μm). (A and C) Quantification of the effect of nocodazole (A) and cytochalasin D (C) treatments on Gem-induced cell elongation; 70 transfected cells were randomly chosen from each sample (nocodazole, cytochalasin D, no drug addition). The percentage of the total cell area covered by the cell body area (*x*-axis in the plots) was calculated for each cell, and the frequency distribution of the values encountered within each sample population was plotted in the above histograms. The corresponding mean values are indicated on the lower left hand corner.

Gem-induced cell spreading requires intact microtubules and actin filaments

The cytoskeleton plays an important role in determining both the morphology and the migratory properties of cells (Waterman-Storer and Salmon, 1999). For this reason, we expected the effect of Gem on cell morphology and dynamics to be cytoskeleton mediated. However, the relative contribution of each cytoskeletal component was not clear. Hence, we tested whether microtubule or actin depolymerization would affect the phenotype induced by Gem overexpression. COS cells transiently transfected with Flag-Gem were incubated overnight with either 10 μM nocodazole or 1 μg/ml cytochalasin D, or left untreated and subsequently fixed (Figure 3). Under those conditions microtubules or microfilaments, respectively, were depolymerized (data not shown).Transfected cells were randomly selected from each sample and subjected to quantification of the cell elongation effect, as described above for Figure 1G. As can be seen in Figure 3, treatment with both drugs had a significant inhibitory effect on Gem-induced formation of long cellular processes: nocodazole (Figure 3A–B) and, to a greater extent, cytochalasin D (Figure 3C–D) treatments caused an increase in the average cell body area/total cell area ratio compared with untreated Gem-expressing cells. These results indicate that both microtubules and actin filaments are involved in Gem-mediated cell shape changes.

Gem associates with both the microtubule and the actin cytoskeleton

Since the above results suggested that Gem might act on both the microtubule and the actin cytoskeleton to alter the cell shape, we analysed whether endogenous Gem colocalized with those cytoskeletal components by immunocytochemistry. For these experiments we chose to use primary cultures of embryonic rat astrocytes because Gem mRNA is remarkably abundant in these cells (Figure 7A). Rat astrocytes were grown on coverslips and then fixed and processed for immunofluorescence with an anti-Gem antibody and either an anti-tubulin (Figure 4A–C) or an anti-actin (Figure 4D–F) antibody. Consistent with our early functional data, the endogenous Gem protein was found partially associated with both microtubules and actin filaments: some of the Gem-positive structures were clearly aligned along microtubules (Figure 4A–C), and most of the actin stress fibres were decorated by Gem staining (Figure 4D–F). The colocalization between Gem and microtubules (less

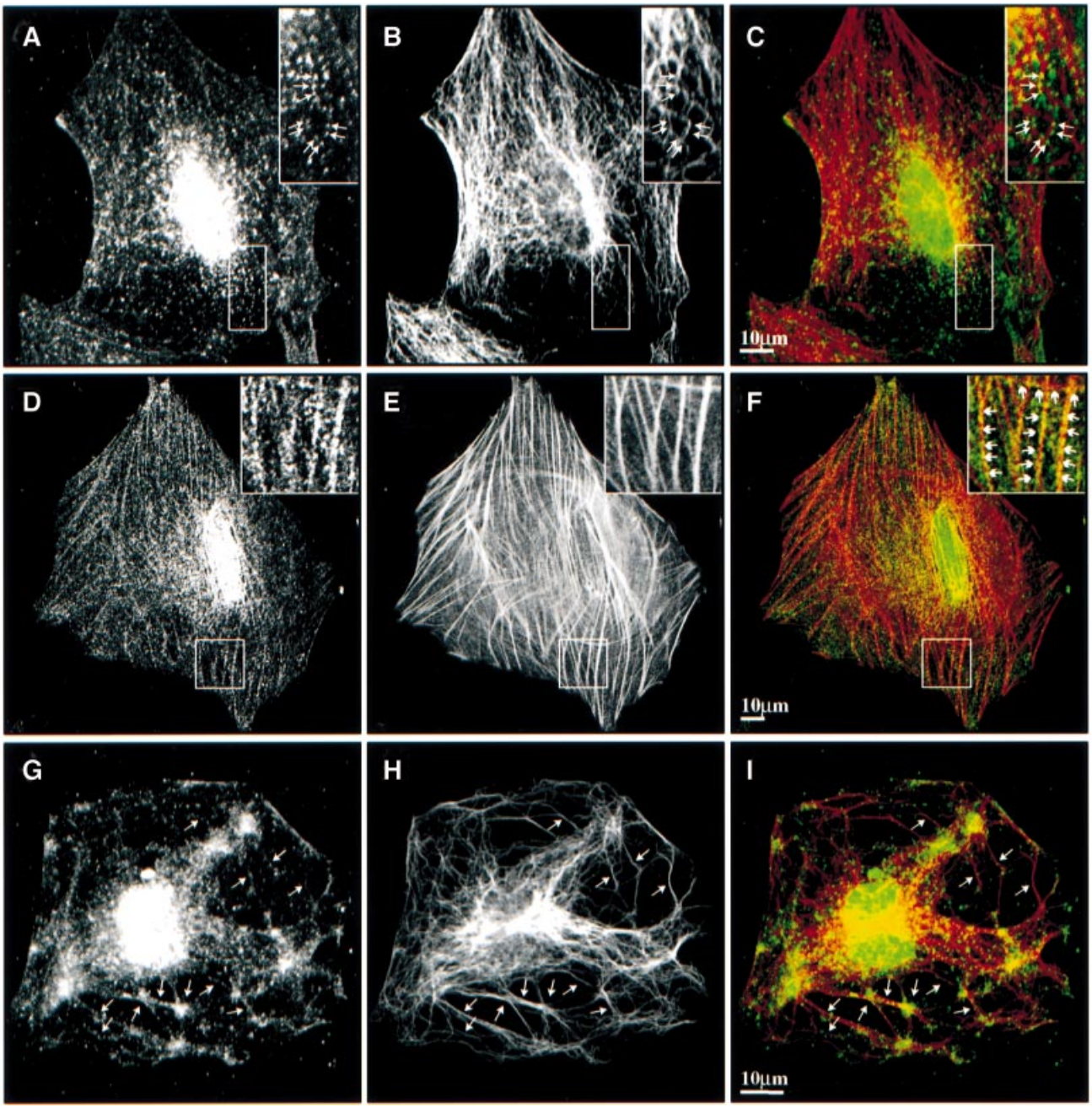

Fig. 4. Gem colocalizes with both microtubules and actin filaments. Primary glial cells were methanol-fixed and double-stained with anti-Gem and either anti-tubulin (A–C and G–I) or anti-actin (D–F) antibodies. (**A–F**) Arrows in (A–C) point at some of the microtubules on which several Gem structures are clearly aligned. Arrows in (F) point at some of the many actin fibres that are decorated by Gem staining. (**G–I**) Cells were treated with 1 μg/ml cytochalasin D for 30 min prior to fixation. Arrows indicate some of the microtubule bundles where Gem is highly enriched. In the merges in (C), (F) and (I), tubulin and actin stainings are shown in red, whereas Gem staining is shown in green.

pronounced than that between Gem and actin) was not due to the fortuitous vicinity of microtubules to actin structures decorated by Gem, because pretreatment of cells with Cytochalasin D caused a striking redistribution of Gem on microtubules rather than a loss of colocalization (Figure 4G–I).

Gem interacts with the novel kinesin-like protein KIF9 by yeast two-hybrid screen

In an attempt to investigate further the interaction of Gem with the cytoskeleton or cytoskeleton-associated proteins, we performed a yeast two-hybrid screen using Gem as bait. Transformation of reporter yeast strains with full-length Gem fused to the Gal4 DNA binding domain yielded only a low number of transformant colonies. This indicated some cytotoxic effect in yeast. The same observation was made with bait constructs comprising C-terminally truncated variants of Gem that lacked either the last seven amino acids (including the cysteine residue at position 290, which is a potential target for lipid modification) or the C-terminal extension (amino acids 266–296), which includes the calmodulin-binding region (data not

shown). Instead, constructs containing only the N-terminal extension (amino acids 1–71) or the GTP-binding core region (amino acids 72–265) revealed normal transformation efficiencies. Thus, we performed yeast two-hybrid screens both with the N-terminal extension and the core region alone. While we did not obtain any putative interaction partner for the N-terminal domain alone after testing of 1.3×10^6 transformants, we could retrieve 227 colonies of putative interaction pairs when we tested 5.4×10^6 transformants with the core region of Gem as bait.

Sequence analysis of the clone that displayed the strongest interaction with Gem produced the partial sequence of a yet unknown protein. Next to the Gal4-activation domain of the library plasmid, this protein contained an open reading frame (ORF) of 411 amino acids, followed by a putative 3′-UTR and a poly A-tail. Cloning of the corresponding full-length cDNA from a murine brain library (see Materials and methods) revealed a protein of 790 amino acids. Following sequence similarity searches, the region corresponding to amino acids 114–245 was seen to contain a perfectly conserved kinesin motor domain. In particular, a partial cDNA clone of 420 nucleotides, published with the name of 'KIF9 motor domain' (Nakagawa *et al*., 1997), was identical to and entirely comprised within our new cDNA sequence. As we had obtained the full-length of the previously partially cloned kinesin-like protein KIF9, we kept the same name for our protein. Figure 5A shows the predicted amino acid sequence of KIF9. The motor domain, located at the N-terminus, shares 40% identity with the corresponding region in conventional kinesin (data not shown). Within the motor domain, highly conserved consensus sequences shared by all known kinesins are found (Figure 5A). The central region of KIF9 contains sequences that have a high probability of forming coiled-coil structures (Figure 5B); therefore, the protein most probably exists as a dimer, as is the case for many other members of the kinesin superfamily. A schematic representation of the major structural features of KIF9 is shown in Figure 5C. Given the N-terminal location of the motor domain, KIF9 is likely to be a plus-ended microtubule motor (Hirokawa *et al*., 1998).

KIF9–Gem interaction is confirmed by immunoprecipitation

Although the interaction between Gem and KIF9 proved to be specific in the yeast two-hybrid system, it had to be verified in mammalian cells. Here the proteins are in their natural environment and at their correct intracellular location. For that purpose, we generated C-terminal hemagglutinin (HA)-tagged mammalian expression vectors encoding full-length KIF9 (KIF9HA), as well as the C-terminal fragment found by the yeast two-hybrid screen [$KIF9_{(379–790)}$–HA].

Cotransfection of Flag-Gem with KIF9HA in HEK-293 cells, followed by immunoprecipitation of Gem from cell lysates and detection of HA-tagged proteins by immunoblotting, revealed a clear and specific interaction between these two proteins in mammalian cells (Figure 6). The interaction was also observed, although to a lower extent, with the C-terminal part of KIF9, consistent with the results from our yeast two-hybrid screen. Control samples overexpressing only KIF9HA did not exhibit any specific band in the western blot, indicating that KIF9 does not bind unspecifically to the anti-Flag affinity beads. Similarly, samples overexpressing only Flag-Gem did not show any band on anti-HA western blots, confirming the specificity of the anti-HA antibody (Figure 6).

Gem–KIF9 interaction did not exhibit a dependence on the nucleotide state of Gem, since addition of the non-hydrolysable GDP and GTP analogues GDPβ-S or GTPγ-S to the cell lysates did not affect the co-immunoprecipitation (data not shown).

To address whether KIF9 was also able to bind other RGK proteins, we tested the ability of KIF9HA and His-tagged Rad (the RGK protein displaying the highest identity with Gem) to interact. However, under the conditions we used no Rad–KIF9 complexes were detected in the Ni-column-purified Rad sample (data not shown), indicating that KIF9 is not a common interacting partner of all RGK proteins. Nevertheless, it cannot be ruled out that KIF9 interacts weakly with other RGK members beside Gem at a level that could not be detected in our coprecipitation experiments.

KIF9 and Gem display identical patterns of gene expression

In order for an interaction between two proteins to be physiologically relevant, it is a prerequisite that the proteins in question are expressed in the same cell at the same time point. We therefore decided to check whether KIF9 and Gem gene expression patterns were compatible with each other.

KIF9 mRNA has a wide but not ubiquitous tissue distribution: it has been detected in brain, kidney, spleen, lung and testis, but seems to be absent from intestine, liver and heart (Nakagawa *et al*., 1997). We first investigated whether KIF9 gene expression was not only spatially but also developmentally regulated. We selected two tissues in which KIF9 has been shown to be expressed, brain and kidney, and analysed the abundance of the corresponding mRNA at different developmental stages by semiquantitative RT–PCR (see Materials and methods). The expression of KIF9 proved indeed to be developmentally regulated (Figure 7B). Its expression was found to be downregulated in the hippocampus at late developmental stages, as lower mRNA levels were detected in the adult tissue than in the embryonic one. Consistently the same downregulation was observed for the corresponding neuronal stages *in vitro* (1 day versus 10 days hippocampal neurons in culture). High expression levels were found in non-neuronal brain cells such as glia. Interestingly, the regulation of KIF9 expression in kidney was opposite to that observed in the hippocampus: zero or very low amounts of mRNA were detected at the embryonic stage, whereas significantly higher levels were found in the adult.

We then examined the relative abundance of Gem mRNA in the same samples, performing semiquantitative PCR analysis with primers specific for the Gem/Kir mRNAs. The results are shown in Figure 7A. Strikingly, the gene expression pattern of Gem was identical to that of KIF9 (compare Figure 7A and B). Gem mRNA was also more abundant in undifferentiated than in differentiated hippocampal neurons, both *in vivo* and *in vitro*; it was also highly represented in glial cells. Finally, it was also expressed more in the adult kidney than in the embryonic

A

```
  1 MGTRKKVQAF VRVRPTDDFA HEMIKYGEDN KSIDIHLKKD  TRRGVVNNQQ TDWSFKLDGV LHNASQDLVY ETVAKDAVSQ  80
 81 ALDGYNGTIM CYGQTGAGKT YTMTGATENY KHRGILPRAL  QQVFRMIEER PTHAITVRVS YLEIYNENLF DLLSTLPYVG 160
161 PSVTPMTIVE NPQGIFIKGL SVHLTSQEED AFSLLFEGET  NRIIASHTMN KNSSRSHCIF TIYMEAHSRT LSDEKYITSK 240
241 INLVDLAGSE RLSKTGSEGR VLKEATYINK SLSFLEQAII  ALGDQNRDHV PFRQSKLTHA LKDSLGGNCN MVLVTNIYGE 320
321 AAQLDETLSS LRFDSRMKLV TTEPAINEKY DAERMVKNLE  KELALLKQEL AIHDSLSNRT LVNYDPMDEI QIAEINSQVR 400
401 RYLEGTLDEI DIINLRQIQE VFNQFRVVLS QQEQEVESAL  RRKYTLIDKN DFAAISAVQK VGLMDIEGNL VGEPDGQSFG 480
481 LGVAPFSVKP GKKPKTKKTP KDQFSSSARK EGASSPVSGK  DFDVASISKT QLIPSSKDGD LKDMLARERE TSSIEPLISD 560
561 SPKEELRAPR PSTPPSRTVA FEEFKNERGS EINRIFKENK  SILNERKKRA SETTQRINAI KQEIDETKDA LNFQKSLREK 640
641 QGEYENKGLM IIDEEEFLLI LKLKDLKKQY RNEYQELRDL  RAEIQYCQRL VDQCRHRLLM EFDIWYNESF MIPEDVQVAL 720
721 KLGSSIRPGM VPISRIVCLG EDDQDRFSHL QQTVLPEGLD  SITFYNAKVK TDQKHNYMKT MVGLQQSHRK           790
```

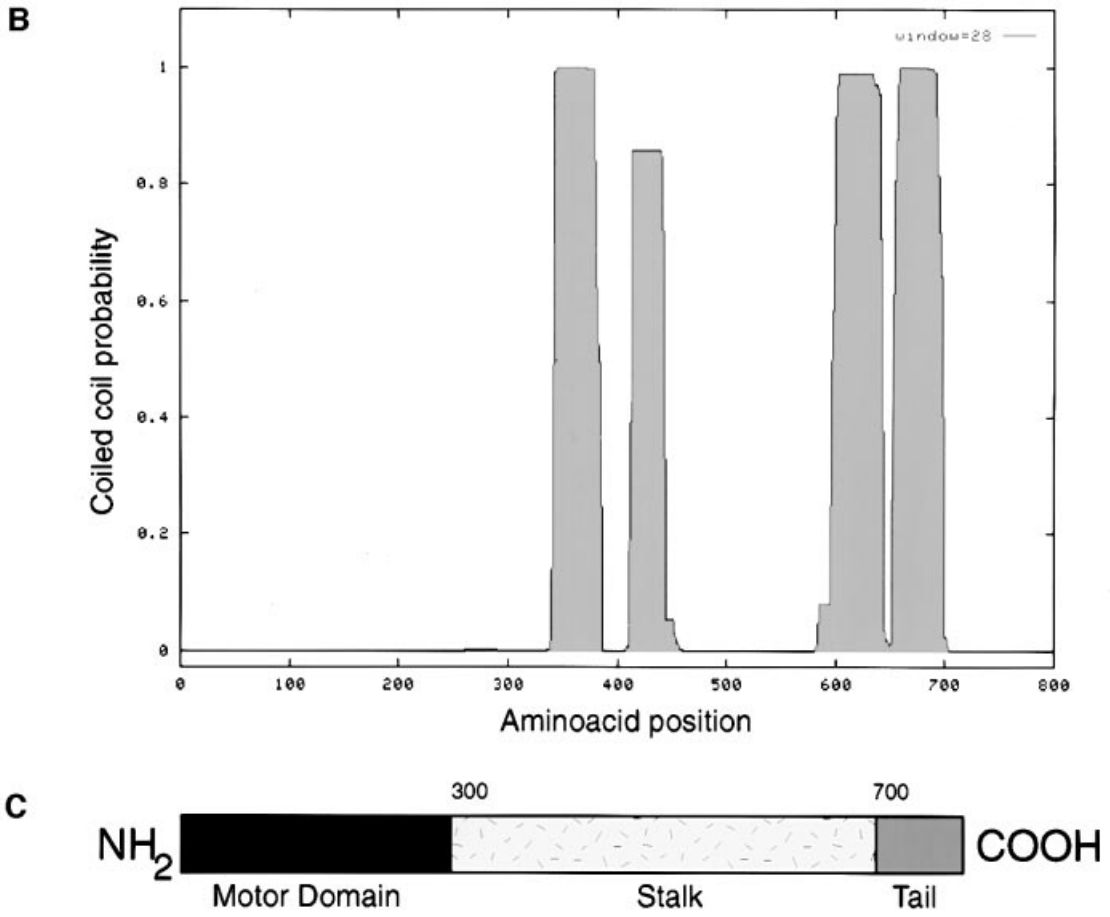

Fig. 5. Primary sequence and structural features of KIF9. (**A**) Predicted amino acid sequence of KIF9. Underlined in black are consensus sequences shared by all known kinesins. These sequence data have been submitted to the EMBL/DDBJ/GenBank databases under accession No. AJ132889. (**B**) Coiled-coil structure prediction. For each amino acid position, the probability of being in a coiled-coil conformation is given according to the program Coils (version 2.2; Lupas *et al*., 1991; Lupas, 1996). The central region of the protein contains two putative coiled-coil domains separated by a broad interruption. (**C**) Schematic representation of KIF9 protein. The globular motor domain is at the N-terminus. The predicted dimerization domain resides in the central stalk region. The putative cargo-binding domain is C-terminal.

one. Thus, the levels of KIF9 and Gem mRNA are regulated in a very coordinated fashion.

Gem and KIF9 associate with membranes and microtubules

In order to gain an insight into the subcellular distribution of KIF9 and Gem, we undertook a biochemical approach. Differential centrifugation of extracts from cells transiently transfected with KIF9HA and Gem constructs showed that the proteins, predicted to be cytosolic according to their amino acid sequence, are not only found in the cytosolic fraction (supernatant) but also in the heavy (10 000 and 20 000 *g* pellets) and light (100 000 *g* pellet) membrane fractions (Figure 8A). KIF9 is particularly enriched in the latter.

Membrane association of both proteins is also suggested by subcellular fractionation on continuous sucrose density gradients (Figure 8B). Isopycnic centrifugation of extracts from cells transiently overexpressing KIF9HA and Gem shows that Gem is mainly enriched in the very light membrane fractions, whereas the motor protein has a distribution with two main peaks—one corresponding to light membrane fractions (as indicated by cofractionation with the light membrane marker caveolin-1), the other

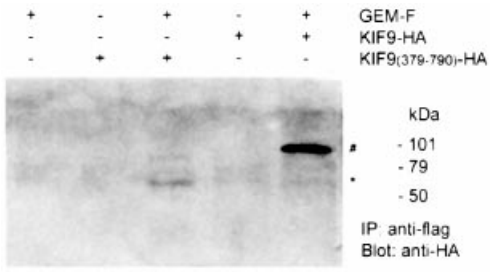

Fig. 6. Co-immunoprecipitation of Gem and KIF9. HEK-293 cells were transiently transfected with Flag-Gem (Gem-F) and KIF9–HA, or the C-terminal part of KIF9 [$KIF9_{(379–790)}$–HA] as indicated. Cell lysates were subjected to co-immunoprecipitation as described in Materials and methods using an anti-Flag affinity matrix followed by immunoblotting with an anti-HA antibody. The positions of full-length KIF9 (#) and of the C-terminal fragment of KIF9 (*) are marked.

corresponding to heavy membrane fractions (as suggested by cofractionation with the heavy membrane marker calnexin).

Finally, we tested the ability both of the putative microtubule motor KIF9 and of Gem (whose association with microtubules had been observed by immunocytochemistry) to bind to the microtubule cytoskeleton biochemically. Both proteins cosedimented specifically with taxol-stabilized microtubules and their presence in the pellet fraction was negligible when microtubule polymerization was inhibited by the addition of the drug nocodazole (Figure 8C).

Discussion

Gem is a member of the RGK family of Ras-like GTPases. Despite the number of years since its original identification (Maguire *et al*., 1994), its function had remained obscure. Here we show that overexpression of Gem induces drastic morphological changes in many cell types, such as HUVEC, COS, HEK-293 and CHO cells. This observation, together with the previous findings that Gem/Kir is upregulated in fully malignant cell lines (Cohen *et al*., 1994; Ross *et al*., 2000) and in mitogen-stimulated T cells (Maguire *et al*., 1994), and that its overexpression induces filamentous growth and invasive properties in yeast (Dorin *et al*., 1995), suggests that Gem might act as oncogene, possibly by positively regulating the migratory properties of cells. Similarly, in the case of Rad in breast cancer cells, there is a correlation between Rad overexpression and increase in colony formation in soft agar and tumour growth in nude mice (Tseng *et al*., 2001).

When investigated dynamically, the elongated phenotype conferred by Gem overexpression is revealed to be the outcome of several abnormal events: cell body retraction, increased fillopodia formation, increased nuclear migration, cortical contraction and, intriguingly, uncoupling between the events taking place at the leading edge and at the trailing edge of cells, which would normally ensure coherent, unidirectional cellular movement. Altogether, these observations suggest that the Gem GTPase can be a general regulator of the cytoskeleton dynamics underlying those processes.

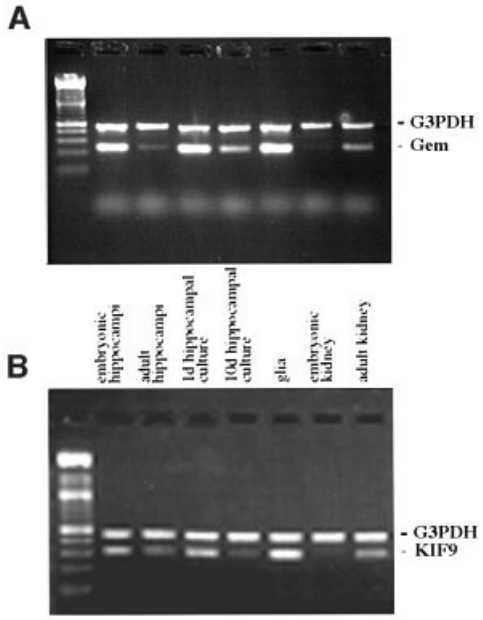

Fig. 7. KIF9 and Gem display the same pattern of gene expression by semiquantitative RT–PCR. cDNA samples from the indicated tissues or cell types were used in PCR reactions with G3PDH primers and either Gem (**A**) or KIF9 (**B**) gene-specific primers. Comparable amounts of cDNA were used in the different PCR reactions as monitored by G3PDH amplification levels.

A role in cell morphology is emerging as a common feature of many RGK family members, as overexpression of Ges and Rem has also been shown to promote a very similar sprouting effect (Pan *et al*., 2000). Surprisingly, although the effect we observed was dramatic, Pan and coworkers found that Gem overexpression did not induce significant morphological changes. One possible explanation for the apparent contradiction between these and our findings may rely on different levels of overexpression: we have observed such a phenotype only in cells that express high levels of exogenous Gem.

Our data start to elucidate the mechanisms by which such profound cellular changes are provoked by Gem: we have shown that Gem-induced cell remodelling relies on both the actin and the microtubule cytoskeleton and, consistently, that Gem is indeed associated with both cytoskeletal components.

A further confirmation of Gem association with the cytoskeleton comes from our finding that Gem interacts with the novel kinesin-like protein KIF9. Gem–KIF9 interaction is proved by several lines of evidence. First, we show that the two proteins interact at a molecular level in a yeast two-hybrid assay. Secondly, Gem–KIF9 interaction is also observed biochemically as the two proteins co-immunoprecipitate. This association does not seem to be mediated by other proteins, since *in vitro* translation–co-immunoprecipitation experiments show that Gem and KIF9 are capable of a weak direct interaction (data not shown). However, we cannot rule out that, *in vivo*, the intervention of a third protein may increase their binding affinity—either by forming a ternary complex or by regulating the interaction via post-translational modification of Gem or KIF9. Thirdly, KIF9 and Gem mRNA

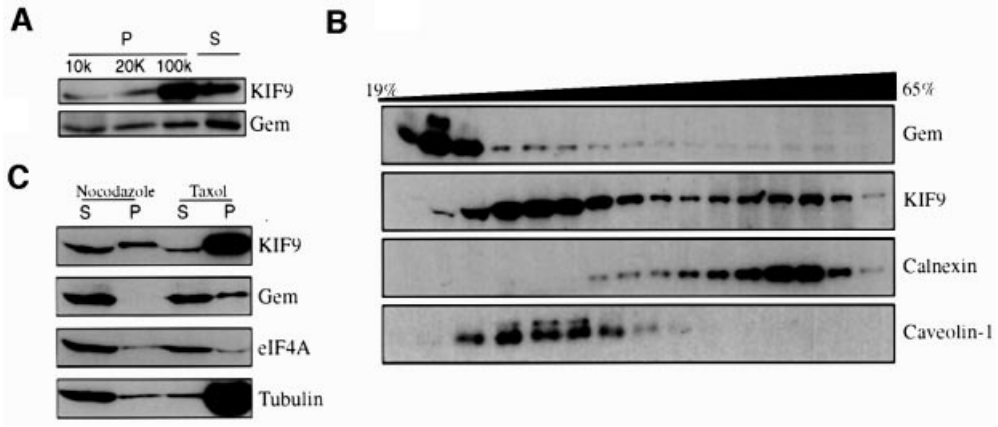

Fig. 8. Biochemical analysis of KIF9 and Gem intracellular distribution. In all of the experiments, KIF9HA was detected with an anti-HA antibody and Gem with an anti-Gem antibody. (**A**) Differential centrifugation experiment. Pellets resulting from the fractionation of an extract from Gem- and KIF9HA-expressing COS cells were probed with an anti-HA and an anti-Gem antibody: lane 1–3: 10 000 *g*, 20 000 *g* and 100 000 *g* pellets, respectively; lane 4, 100 000 *g* supernatant. (**B**) Distribution of Gem and KIF9HA on continuous sucrose density gradients. The fractionation of the light membrane marker caveolin-1 and of the heavy membrane marker calnexin are shown as the control of proper membrane separation. Gem was mainly enriched in the light membrane fractions (peak at 25%). KIF9 was detected in several fractions. Its distribution had two main peaks at 35 and 56% w/v, respectively. (**C**) Microtubule cosedimentation assay. KIF9HA and Gem stay mainly soluble (S) when microtubule polymerization is inhibited by the addition of nocodazole (lanes 1–2) and are specifically recovered in the pellet (P) in the presence of taxol-stabilized microtubules (lanes 3–4). The behaviour of tubulin and of the translation initiation factor eIF4A are shown as positive and negative controls, respectively.

display identical patterns of gene expression. The striking similarity between their expression patterns suggests that KIF9 and Gem are involved in a common cellular process, and the way cells have chosen to activate or inactivate this function is by transcriptionally regulating the expression of the proteins responsible for it. Moreover, the high Gem–KIF9 levels found during neuronal growth and differentiation, together with Gem's implication in cell elongation, raise the interesting possibility of an involvement of these two proteins in neuronal development.

The biochemical analysis of KIF9 and Gem cellular distributions reveals interesting results. Although both proteins are predicted to be cytosolic according to their primary sequence, they are mainly bound to membranes—as indicated by their profile in differential centrifugation and sucrose density gradient experiments. The results from those experiments also suggest that only a small proportion of KIF9 and Gem are found in a complex in cells, since the two proteins display overlapping but different fractionation patterns in the density gradient. Moreover, KIF9 cofractionation with heavy and light membranes suggests that this motor protein is associated with two different organelles. Further studies will be needed to identify them.

KIF9 was isolated in an attempt to find partners of Gem that would elucidate the molecular mechanism of Gem association with the cytoskeleton. Two observations make the Gem-interacting partner KIF9 a likely candidate for recruiting this GTPase on microtubules. On the basis of its amino acid sequence, KIF9 is a putative microtubule motor and, as shown by our microtubule sedimentation assay, it is a microtubule-associated protein (MAP). However, the motor protein function of KIF9 does not seem to be essential for the Gem-induced phenotypic changes. When we overexpressed a rigor mutant of KIF9 bearing a single T100N point mutation in the ATP binding site, and analogous to the T93N conventional kinesin rigor mutant (Nakata and Hirokawa, 1995), we were unable to see significant differences in Gem-induced cell elongation (data not shown). Nevertheless, the possibility of an involvement of KIF9 in Gem-induced cell shape changes cannot at present be ruled out.

Our finding that a member of the small GTPase family interacts with a kinesin-like protein is of biological relevance. A growing number of such interactions is being described in the literature: rab6 directly binds rabkinesin6 (Echard *et al*., 1998), Rho, Rac and cdc42 have been found to interact with the kinesin-associated protein kinectin (Hotta *et al*., 1996).

What might be the role of KIF9–Gem interaction? Gem might simply be regulating the motor activity of KIF9, as already proposed for rab6 on rabkinesin6 (Echard *et al*., 1998). Alternatively, if Gem is found to interact with actin-binding proteins, as suggested by our colocalization data with actin and by the fact that such an interaction has been demonstrated for the closely related Rad (Zhu *et al*., 1996), the ternary complex between Gem, KIF9 and an actin-binding protein may function in bridging the microtubule and the actin cytoskeleton together. A third possibility is that the binding of Gem to KIF9 would be a way to recruit it on microtubules in the vicinity of its effectors/regulators. Support for this hypothesis comes from the interesting observation that NM23, a protein that has been shown to have GEF properties on Gem *in vitro* (Zhu *et al*., 1999), also localizes to microtubules (Biggs *et al*., 1990). Growing evidence suggests that microtubules can act as signal transduction platforms: key components of the hedgehog signalling pathway are recruited to microtubules through the kinesin-like protein costal2 (Robbins *et al*., 1997; Sisson *et al*., 1997); the MAP kinase MLK2, effector of Rac and cdc42 in the signalling cascade that leads to c-Jun N-terminal kinase (JNK) activation, is localized together with JNK on microtubules via the interaction with the kinesin-like protein KIF3

(Nagata *et al*., 1998); Rac itself can be recruited on microtubules through the binding with Lfc and can thereby activate its signalling targets (Glaven *et al*., 1999).

The data that we present open the way to an understanding of the cellular function of Gem and to the molecular dissection of the Gem signalling pathway(s).

Materials and methods

Cell lines and primary cultures

COS cells were grown in Dulbecco's modified Eagle's medium (DMEM) containing 10% fetal calf serum (Gibco-BRL), 2 mM glutamine and penicillin (100 U/ml)/streptomycin (100 μg/ml), and maintained at 37°C and 5% CO_2. HUVEC were grown as described elsewhere (Stehlik *et al*., 1998). HEK-293 cells were grown as described in Schmid *et al*. (2000). Primary cultures of hippocampal neurons and of glial cells were prepared according to the protocols of Goslin and Banker (1991).

Drug treatment and transient transfections were performed as described in the Supplementary data, available at *The EMBO Journal* Online.

Immunocytochemistry

Cells were grown for 18–24 h on glass coverslips, rinsed with phosphate-buffered saline (PBS) and fixed either in ice-cold methanol for 5 min or in 4% paraformaldehyde for 10 min. Immunofluorescence labelling was performed as described in Santama *et al*. (1998). The following primary antibodies were used: mouse anti-Gem P2D10 (1:100; Maguire *et al*., 1994; a gift from K.Kelly); rabbit anti-tubulin (1:100, a gift from E.Karsenti); rabbit anti-actin (1:20, Sigma); M1 mouse anti-Flag (1:500, Sigma). For the anti-Gem antibody, a sandwich of secondary antibodies was required [fluoroescein isothiocyante (FITC)-conjugated sheep anti-mouse followed by FITC-conjugated donkey anti-sheep]. Image acquisition, live cell imaging and quantification of the Gem phenotype are described in the Supplementary data.

Two-hybrid screening

The yeast two-hybrid screening was performed with components of the Matchmaker Two-Hybrid System 2 (Clontech, Palo Alto, CA). The core region of Gem (amino acids 72–265) was cloned by PCR (forward primer: 5′-AAAACCATGGGGAACACCTACTACCG-3′; reverse primer: 5′-TTTTGAATTCTATTTCCTGGGCATGCTCTC-3′) in-frame into the Gal4BD-containing bait vector (*pAS*2-1; Clontech) using the *Nco*I and *Eco*RI sites. The resulting construct was verified by sequencing. Further details of the two-hybrid screen procedure are given in the Supplementary data.

The two-hybrid screen was performed using a library from phyto-hemagglutinin (PHA)-stimulated leukocytes (Clontech; HL4021AB). About 5.4×10^6 transformants were screened yielding 227 positive colonies; 14 colonies with high *lacZ* expression were analysed further. Yeast DNA was prepared by the method of Liang and Richardson (1992), followed by electro-transformation into HB101 bacteria. Sequence analysis of the strongest *lacZ*-positive interaction partner of Gem revealed the partial cDNA sequence of a yet unknown protein.

Cloning of full-length KIF9 cDNA

To obtain the full-length cDNA sequence of the newly identified Gem interacting protein we performed 5′ and 3′ rapid amplification of cDNA ends (RACE) reactions using the Mouse Brain Marathon-Ready cDNA kit (Clontech Laboratories Inc., Palo Alto, CA). Since we had used a human library for the two-hybrid screen and our RACE library was from mouse, we first obtained the murine equivalent of the partial human clone obtained by two-hybrid. Primers selected from the ORF of the human partial cDNA sequence (forward: GCACCTTTGTGACCTATGACCCCATGG; reverse: TTTTCTGTGTGACTGTTGGAGGCCCA) PCR amplified a murine cDNA fragment, which upon sequencing was shown to be 82.7% identical to its human counterpart.

The RACE reactions were performed according to the manufacturer's instructions. The reaction program used was Program 1 of the User Manual. Advantage KlenTaq Polymerase Mix (Clontech Laboratories Inc., Palo Alto, CA). The 3′ end RACE reaction produced different identical clones whose sequence overlapped at the 5′ end with our partial cDNA clone and contained a stop codon, a 3′ UTR and a poly-A tail. From the 5′ end RACE reaction, it was possible to isolate some clones whose sequence overlapped at the 3′ end with our partial cDNA clone and contained the beginning of the ORF at the 5′ end (a start codon that was preceded by an in-frame stop codon).

The full-length cDNA clone of KIF9 was then obtained performing a PCR with the following pair of primers: CCTCAAGTTGCTGCAGTTCTAGCGGTC and GCAAGGGTGTCCTTTGGAGGATGCTCATCC. The reaction programme and conditions were the same as used for RACE except for the template cDNA, which was from isolated mouse embryonic hippocampi. The PCR product was cloned in *pCR*2.1; upon sequencing, two clones were confirmed to contain the whole KIF9 ORF.

Gem and KIF9 mammalian expression vectors

Relevant features of the Gem and KIF9 mammalian expression vectors used in this study can be found in the Supplementary data.

Isolation of mRNA

Poly(A)$^+$ RNA was affinity purified with a QuickPrep Micro mRNA purification kit (Pharmacia Biotech, Sweden) from hippocampal neurons in culture (1 and 10 days old), glia primary cultures and isolated hippocampi. Mouse embryonic (E17) and adult kidney mRNAs were a kind gift of Marino Zerial.

RT–PCR

cDNA synthesis was performed using ~10 ng of mRNA and the MMLV reverse transcriptase (Advantage RT-for-PCR kit Clontech Laboratories Inc., Palo Alto, CA). Specific primer pairs were designed to monitor KIF9 (forward: ACCATGACAGGGGCAACGGAGAATTACAAGC; reverse: GGAGGCAATGATC CTGTTGGTCTCGCC) and Gem/KIR (forward: ATGACTCTGAATAATGTCACCATGCCGCCAA; reverse: ATAAGCACTACTCGGTAGTAGGTGTTTCCA) expression by PCR amplification. The PCR reactions contained: ~1 ng cDNA, 10 nmol of each dNTP, 1 unit of AmpliTaq DNA polymerase (Perkin-Elmer) and 20 pmol of each primer in 1× Perkin-Elmer PCR buffer (containing 1.5 mM $MgCl_2$) in a total volume of 50 μl. The PCR amplification consisted of 33 cycles of: (i) 10 s at 94°C, (ii) 10 s at 60°C and (iii) 35 s at 72°C. To obtain a semiquantitative analysis, primers specific for the glyceraldehyde-phosphate dehydrogenase (GAPDH) housekeeping gene (20 pmol each) were added to the PCRs; the GAPDH cDNA was used as internal standard to normalize the concentration of the different cDNA samples. As the GAPDH mRNA was more abundant than the KIF9 or Gem mRNA, KIF and Gem cDNAs were allowed to undergo five initial cycles of amplification before the GAPDH primers were added. Under these PCR conditions, none of the cDNAs was amplified to saturation.

Co-immunoprecipitation

HEK-293 transiently transfected with Flag-Gem and/or KIF9HA, or the C-terminal part of KIF9 [$KIF9_{(379–790)}$-HA] were lysed for 15 min at 4°C with lysis buffer (0.5% NP-40, 50 mM Tris–HCl pH 7.5, 1 mM EDTA, 150 mM NaCl and including protease inhibitors: 10 μg/ml aprotinin, 20 μg/ml phosphoramidon, 40 μg/ml pefabloc, 1 μg/ml leupeptin, 1 μg/ml pepstatin). The extracts were centrifuged for 15 min at 14 000 *g* at 4°C. The supernatants were diluted with an equal volume of ice-cold PBS before adding 15 μl of an anti-Flag affinity matrix (Sigma), followed by rotating incubation at 4°C for 2 h. The beads were washed four times with ice-cold PBS and the bound material was eluted in SDS–PAGE buffer. A list of the primary antibodies used in this and the following biochemical experiments can be found in the Supplementary data.

Subcellular fractionation

PNS (post-nuclear supernatant) preparation. COS cells transiently transfected with pMT2TGem and pcKIF9HA (one confluent 15 cm dish) were washed twice with PBS and scraped in MEPS buffer (5 mM $MgSO_4$, 5 mM EGTA, 35 mM K$^+$PIPES pH 7.1, 1 mM dithiothreitol, 0.2 M sucrose) plus 1 mM 4-(amidino-phenyl)-methane sulfonyl fluoride (APMSF) and a mix of protease inhibitors (20 μg/ml aprotinin, chymostatin, pepstatin and leupeptin). The sample was homogenized and centrifuged at 800 *g* for 10 min. The resulting PNS was subjected to differential centrifugation steps (10–20–100 000 *g* for 30 min each), pellets were recovered from the three fractions, the supernatant from the last centrifugation step was precipitated with trichloroacetic acid (TCA) and regarded as the cytosolic fraction. Comparable protein amounts were subjected to SDS–PAGE and western blotting.

Sucrose density gradient sedimentation

PNS from COS cells transiently transfected with pMT2TGem and pcKIF9HA (seven confluent 15 cm dishes) was obtained as described above, loaded on top of a 20–60% continuous sucrose gradient and centrifuged at 35 000 rpm for 16 h at 4°C in a SW40 rotor. The gradient

was divided into 16 fractions collected from the top of the tube. After the sucrose density of each fraction had been measured, they were precipitated with TCA. Equal sample volumes were subjected to SDS–PAGE and western blotting.

Microtubule cosedimentation assay

PNS from COS cells transiently transfected with pMT2TGem and pcKIF9HA (two confluent 15 cm dishes) was prepared as described above, with the exception that the buffer used was BRB80 (80 mM K^+PIPES pH 6.8, 1 mM $MgCl_2$, 1 mM EGTA). The sample was supplemented with 1 μg/ml cytochalasin D and incubated for 30 min at 4°C. The extract was then clarified by centrifugation at 165 000 *g* for 20 min. The supernatant was split in two samples: one (N) was supplemented with 40 μM nocodazole and kept on ice; the other (T) was supplemented with 2 mM GTP, 2 mM $MgCl_2$ and 20 μM taxol and incubated for 30 min at 33°C. AMP-PNP (1.5 mM) was added to the T sample, which was subsequently incubated for 20 min at room temperature. Both samples were spun through a 15% sucrose cushion at 165 000 *g* for 20 min at 25°C. The resulting pellets were resuspended in SDS–PAGE loading buffer, the supernatants were precipitated with methanol/chloroform and resuspended in SDS–PAGE loading buffer. Pellets were entirely loaded on the gel, whereas only 1/10 of the supernatant was loaded.

Supplementary data

Supplementary data for this paper are available at *The EMBO Journal* Online.

Acknowledgements

We thank Aspasia Ploubidou, Rafael Edgardo Carazo-Salas and Marino Zerial for critical reading of the manuscript as well as for scientific advice and discussion. Special thanks go to Michael Way for intensive and fruitful discussion as well as for his generosity in providing reagents. We also thank Dimuthu deSilva for the GemS89N construct, Kathleen Kelly for the P2D10 anti-Gem monoclonal antibody and the pMT2TGem construct, and Bianca Hellias and Peter Gold for technical assistance. This work was partially funded by the Competence Center for Biomolecular Therapeutics, Vienna, Austria.

References

Biggs,J., Hersperger,E., Steeg,P.S., Liotta,L.A. and Shearn,A. (1990) A *Drosophila* gene that is homologous to a mammalian gene associated with tumor metastasis codes for a nucleoside diphosphate kinase. *Cell*, **63**, 933–940.

Bilan,P.J., Moyers,J.S. and Kahn,C.R. (1998) The Ras-related protein Rad associates with the cytoskeleton in a non-lipid-dependent manner. *Exp. Cell Res.*, **242**, 391–400.

Bourne,H.R., Sanders,D.A. and McCormick,F. (1991) The GTPase superfamily: conserved structure and molecular mechanism. *Nature*, **349**, 117–127.

Cohen,L. *et al.* (1994) Transcriptional activation of a Ras-like gene (kir) by oncogenic tyrosine kinases. *Proc. Natl Acad. Sci. USA*, **91**, 12448–12452.

Dorin,D., Cohen,L., Del Villar,K., Poullet,P., Mohr,R., Whiteway,M., Witte,O. and Tamanoi,F. (1995) Kir, a novel Ras-family G-protein, induces invasive pseudohyphal growth in *Saccharomyces cerevisiae*. *Oncogene*, **11**, 2267–2271.

Echard,A., Jollivet,F., Martinez,O., Lacapere,J.J., Rousselet,A., Janoueix-Lerosey,I. and Goud,B. (1998) Interaction of a Golgi-associated kinesin-like protein with Rab6. *Science*, **279**, 580–585.

Feig,L.A. (1999) Tools of the trade: use of dominant-inhibitory mutants of Ras-family GTPases. *Nature Cell Biol.*, **1**, E25–E27.

Finlin,B.S. and Andres,D.A. (1997) Rem is a new member of the Rad- and Gem/Kir Ras-related GTP-binding protein family repressed by lipopolysaccharide stimulation. *J. Biol. Chem.*, **272**, 21982–21988.

Finlin,B.S., Shao,H., Kadono-Okuda,K., Guo,N. and Andres,D.A. (2000) Rem2, a new member of the Rem/Rad/Gem/Kir family of Ras-related GTPases. *Biochem. J.*, **347**, 223–231.

Fischer,R., Wei,Y., Anagli,J. and Berchtold,M.W. (1996) Calmodulin binds to and inhibits GTP binding of the Ras-like GTPase Kir/Gem. *J. Biol. Chem.*, **271**, 25067–25070.

Glaven,J.A., Whitehead,I., Bagrodia,S., Kay,R. and Cerione,R.A. (1999) The Dbl-related protein, Lfc, localizes to microtubules and mediates the activation of Rac-signaling pathways in cells. *J. Biol. Chem.*, **274**, 2279–2285.

Goslin,K. and Banker,G. (1991) Rat hippocampal neurons in low density. In Goslin,K. and Banker,G. (eds), *Culturing Nerve Cells*. MIT Press, Cambridge, MA.

Hirokawa,N., Noda,Y. and Okada,Y. (1998) Kinesin and dynein superfamily proteins in organelle transport and cell division. *Curr. Opin. Cell Biol.*, **10**, 60–73.

Hotta,K., Tanaka,K., Mino,A., Kohno,H. and Takai,Y. (1996) Interaction of the Rho family small G proteins with kinectin, an anchoring protein of kinesin motor. *Biochem. Biophys. Res. Commun.*, **225**, 69–74.

Liang,Q. and Richardson,T. (1992) A simple and rapid method for screening transformant yeast colonies using PCR. *Biotechniques*, **13**, 730–732.

Lupas,A. (1996) Coiled coils: new structures and new functions. *Trends Biochem. Sci.*, **21**, 375–382.

Lupas,A., Van Dyke,M. and Stock,J. (1991) Predicting coiled coils from protein sequences. *Science*, **252**, 1162–1164.

Maguire,J., Santoro,T., Jensen,P., Siebenlist,U., Yewdell,J. and Kelly,K. (1994) Gem: an induced, immediate early protein belonging to the Ras family. *Science*, **265**, 241–244.

Moyers,J.S., Bilan,P.J., Zhu,J. and Kahn,C.R. (1997) Rad and Rad-related GTPases interact with calmodulin and calmodulin-dependent protein kinase II. *J. Biol. Chem.*, **272**, 11832–11839.

Moyers,J.S., Zhu,J. and Kahn,C.R. (1998) Effects of phosphorylation on function of the Rad GTPase. *Biochem. J.*, **333**, 609–614.

Nagata,K., Puls,A., Futter,C., Aspenstrom,P., Schaefer,E., Nakata,T., Hirokawa,N. and Hall,A. (1998) The MAP kinase, MLK2, colocalizes with activated JNK along microtubules and associates with kinesin superfamily motor KIF3. *EMBO J.*, **17**, 149–158.

Nakagawa,T., Tanaka,Y., Matsuoka,E., Kondo,S., Okada,Y., Noda,Y., Kanai,Y. and Hirokawa,N. (1997) Identification and classification of 16 new kinesin superfamily (KIF) proteins in mouse genome [published erratum appears in *Proc. Natl Acad. Sci. USA*, 1999, **96**, 4214]. *Proc. Natl Acad. Sci. USA*, **94**, 9654–9659.

Nakata,T. and Hirokawa,N. (1995) Point mutation of adenosine triphosphate-binding motif generated rigor kinesin that selectively blocks anterograde lysosome membrane transport. *J. Cell Biol.*, **131**, 1039–1053.

Pan,J.Y., Fieles,W.E., White,A.M., Egerton,M.M. and Silberstein,D.S. (2000) Ges, a human GTPase of the Rad/Gem/Kir family, promotes endothelial cell sprouting and cytoskeleton reorganization. *J. Cell Biol.*, **149**, 1107–1116.

Reynet,C. and Kahn,C.R. (1993) Rad: a member of the Ras family overexpressed in muscle of type II diabetic humans. *Science*, **262**, 1441–1444.

Robbins,D.J., Nybakken,K.E., Kobayashi,R., Sisson,J.C., Bishop,J.M. and Therond,P.P. (1997) Hedgehog elicits signal transduction by means of a large complex containing the kinesin-related protein costal2. *Cell*, **90**, 225–234.

Ross,D.T. *et al.* (2000) Systematic variation in gene expression patterns in human cancer cell lines. *Nature Genet.*, **24**, 227–235.

Santama,N., Krijnse-Locker,J., Griffiths,G., Noda,Y., Hirokawa,N. and Dotti,C.G. (1998) KIF2β, a new kinesin superfamily protein in non-neuronal cells, is associated with lysosomes and may be implicated in their centrifugal translocation. *EMBO J.*, **17**, 5855–5867.

Schmid,J.A., Birbach,A., Hofer-Warbinek,R., Pengg,M., Burner,U., Furtmuller,P.G., Binder,B.R. and de Martin,R. (2000) Dynamics of NFκB and IκBα studied with green fluorescent protein (GFP) fusion proteins. Investigation of GFP–p65 binding to DNA by fluorescence resonance energy transfer. *J. Biol. Chem.*, **275**, 17035–17042.

Sisson,J.C., Ho,K.S., Suyama,K. and Scott,M.P. (1997) Costal2, a novel kinesin-related protein in the hedgehog signaling pathway. *Cell*, **90**, 235–245.

Stehlik,C., de Martin,R., Kumabashiri,I., Schmid,J.A., Binder,B.R. and Lipp,J. (1998) Nuclear factor (NF)-κB-regulated X-chromosome-linked *iap* gene expression protects endothelial cells from tumor necrosis factor α-induced apoptosis. *J. Exp. Med.*, **188**, 211–216.

Tseng,Y.H., Vicent,D., Zhu,J., Niu,Y., Adeyinka,A., Moyers,J.S., Watson,P.H. and Kahn,C.R. (2001) Regulation of growth and tumorigenicity of breast cancer cells by the low molecular weight GTPase Rad and nm23. *Cancer Res.*, **61**, 2071–2079.

Vanhove,B., Hofer-Warbinek,R., Kapetanopoulos,A., Hofer,E., Bach, F.H. and de Martin,R. (1997) Gem, a GTP-binding protein from

mitogen-stimulated T cells, is induced in endothelial cells upon activation by inflammatory cytokines. *Endothelium*, **5**, 51–61.

Waterman-Storer,C.M. and Salmon,E. (1999) Positive feedback interactions between microtubule and actin dynamics during cell motility. *Curr. Opin. Cell Biol.*, **11**, 61–67.

Zhu,J., Reynet,C., Caldwell,J.S. and Kahn,C.R. (1995) Characterization of Rad, a new member of Ras/GTPase superfamily and its regulation by a unique GTPase-activating protein (GAP)-like activity. *J. Biol. Chem.*, **270**, 4805–4812.

Zhu,J., Bilan,P.J., Moyers,J.S., Antonetti,D.A. and Kahn,C.R. (1996) Rad, a novel Ras-related GTPase, interacts with skeletal muscle β-tropomyosin. *J. Biol. Chem.*, **271**, 768–773.

Zhu,J., Tseng,Y.H., Kantor,J.D., Rhodes,C.J., Zetter,B.R., Moyers,J.S. and Kahn,C.R. (1999) Interaction of the Ras-related protein associated with diabetes Rad and the putative tumor metastasis suppressor NM23 provides a novel mechanism of GTPase regulation. *Proc. Natl Acad. Sci. USA*, **96**, 14911–14918.

Received December 1, 2000; revised May 28, 2001; accepted June 12, 2001